

# Calcareous nannofossil distribution in the upper Maastrichtian–lower Thanetian interval in the Izeh zone (Southwest Iran): biostratigraphic framework and stage boundary identification in the Eastern Tethys

Saeedeh Senemari<sup>1\*</sup>, Fabrizio Frontalini<sup>2</sup>, Arman Jafarian<sup>3</sup> and Marziyeh Notghi Moghaddam<sup>4</sup>

<sup>1</sup>Department of Mining, Imam Khomeini International University, Qazvin, Iran

<sup>2</sup>Dipartimento di Scienze Pure e Applicate (DiSPeA), Università degli Studi di Urbino “Carlo Bo”, Campus Scientifico, Località Crocicchia, Urbino 61029, Italy

<sup>3</sup>State Key Laboratory of Biogeology and Environmental Geology, China University of Geosciences, Beijing 100083, China

<sup>4</sup>Department of Geology, Faculty of Science, Payame Noor University, Tehran, Iran

\*Corresponding author: senemari2004@yahoo.com; S.Senemari@eng.ikiu.ac.ir

**ABSTRACT:** The distribution of calcareous nannofossil species in the upper part of Gurpi Formation and lower part of Pabdeh Formation has been investigated in the Karta section (northwest of Izeh in Zagros Basin, Iran, Eastern Tethys) to provide a biostratigraphic framework from Maastrichtian to Thanetian interval. In this study, 31 genera and 52 species of calcareous nannofossils have been identified and based on the recognized bioevents and the resulting biozones, the studied interval spans from the top of the nannofossil zone UC19<sup>TP</sup> to the base of the NP7 zone and covers ~10.8 Myr. In this study, the Gurpi Formation spans from the upper UC19<sup>TP</sup> to NP4 zones, while the lowest part of Pabdeh Formation covers NP5, NP6 and NP7 zones. The studied sequence is continuous and encompasses Cretaceous–Paleogene (K/Pg), Danian/Selandian and Selandian/Thanetian boundaries. The K/Pg boundary is characterized by nannofossil assemblage recognized worldwide, such as the occurrence of *Biantholithus*, *Cruciplacolithus*, *Braarudosphaera*, *Praeprinsius*, and calcareous blooms of *Thoracosphaera* spp. A decrease in the abundance of nannofossils is observed in the upper part of the Maastrichtian to the lower part of the Danian; poor to moderate preservation of nannofossils and low diversified nannofossil assemblages cover most of the studied samples. Here, as a result of species poor to moderate preservation, we observe patterns of stepwise extinctions upward in the top of CC25 zone, that culminate with the last occurrence of eight species, just prior to the base of the UC20b<sup>TP</sup>. We interpret these patterns to be mainly the result of diagenetic alteration. Our dataset provides a record over a long-lasting interval of stepwise extinctions toward the K/Pg boundary that was likely caused by the diagenetically-enhanced Signor-Lipps effect.

**Keywords:** Gurpi-Pabdeh formations, Biozones, Nannofossils, Cretaceous, Maastrichtian–Paleocene, Zagros Basin

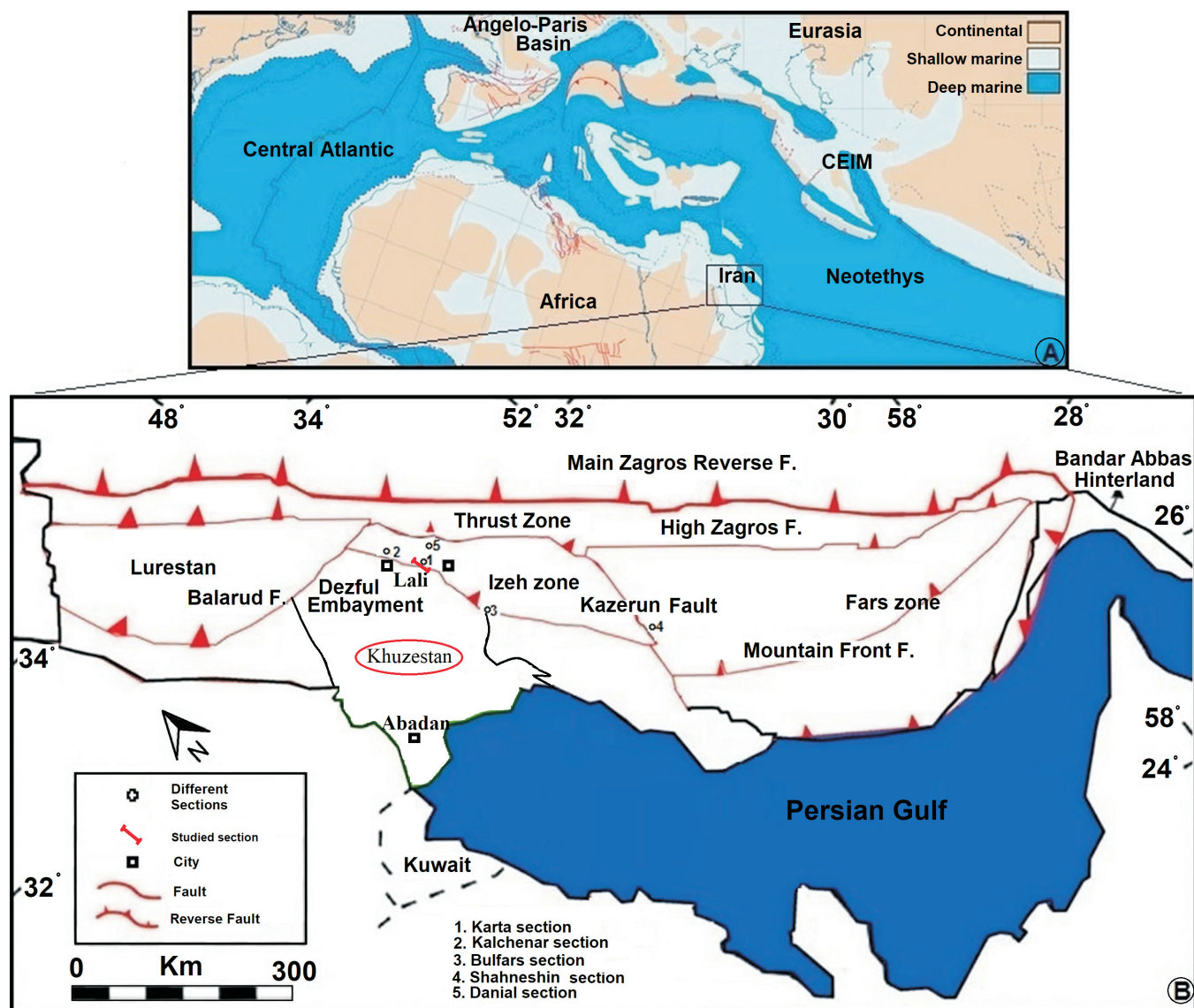
## INTRODUCTION

Numerous biostratigraphic, paleoclimatic and paleoenvironmental investigations have been performed on the Late Cretaceous and early Paleogene interval worldwide (e.g., Martini 1971; Sissingh 1977; Perch-Nielsen 1985; Coccioni et al. 2012; Agnini et al. 2014). Most of the existing records are from central Tethys localities, where several standard biostratigraphic schemes have also been calibrated and developed (e.g. Agnini et al. 2014). The Eastern Tethys (e.g. Zagros Basin) represents an important part of the Tethyan Realm and had a direct connection with the Indian Ocean (Mohammadkhani et al. 2022), but it has been comparatively less studied than the central-western Tethys (e.g. Renne et al. 2013; Thibault et al. 2016; Thibault 2017; Mateo et al. 2017; Farouk et al. 2018). In fact, although Cretaceous to Paleogene deposits extensively crop out in the southwestern Iran (Eastern Tethys), sedimentary data from the Zagros Basin are comparatively fewer when compared with other regions of the world (Ghasemi-Nejad et al. 2006; Etemad et al. 2008; Senemari and Azizi 2012; Beiranvand et al. 2013). In this regard, standard Late Cretaceous and Paleogene biostratigraphic schemes have been developed in the areas such as the central Tethyan, Atlantic, Pacific Oceans (e.g. Coccioni and Premoli-Silva 2015). In order to examine the reliable appli-

cation of these schemes in the Eastern Tethys, it is necessary to provide new biostratigraphic records in relatively neglected areas such as the Zagros Basin.

Several studies have been carried out in the Zagros Basin by oil companies and researchers on different aspects of stratigraphy including biostratigraphy based on foraminifera, palynomorphs and calcareous nannofossils (e.g. James and Wynd 1965; Darvishzadeh et al. 2007; Babazadeh et al. 2009; Hadavi and Senemari 2010; Senemari et al. 2010; Afghah and Ghiyasi 2013). These studies mostly rely on records representing lateral variations in thickness, environmental conditions, and age of the Gurpi Fm. (Parandavar et al. 2013; Beiranvand et al. 2014; Razmjooei et al. 2014; 2018; Senemari and Foroughi 2019; Senemari and Afghah 2020). Most of the researches have focused on the Cretaceous–Paleogene (K/Pg) transition, which has undoubtedly been an important target interval in the Zagros Basin (e.g. Ezampanah et al. 2018; Rostami et al. 2018, 2020).

In our effort to study the biostratigraphy of the K/Pg interval at a previously unstudied locality (Karta section, Khuzestan province, southwestern Iran), we discovered special features in the nannofossil assemblage that are unlike any other documented K/Pg records worldwide. Our dataset documents a stepwise ex-



TEXT-FIGURE 1

(A) The Late Cretaceous paleogeography of the Middle East (after Wilmsen et al. 2015) and (B) the location geological map of the Zagros Basin together with the approximate location of several studied sites (modified and adapted from Sherhati and Letouzey 2004).

tion of calcareous nannofossil assemblages during the K/Pg transition, possibly caused by the diagenetic Signor-Lipps effect. The present study aims to establish a biostratigraphic framework based on calcareous nannofossils, to investigate the K/Pg boundary and to correlate the Karta section with other regional successions that cover a similar time span.

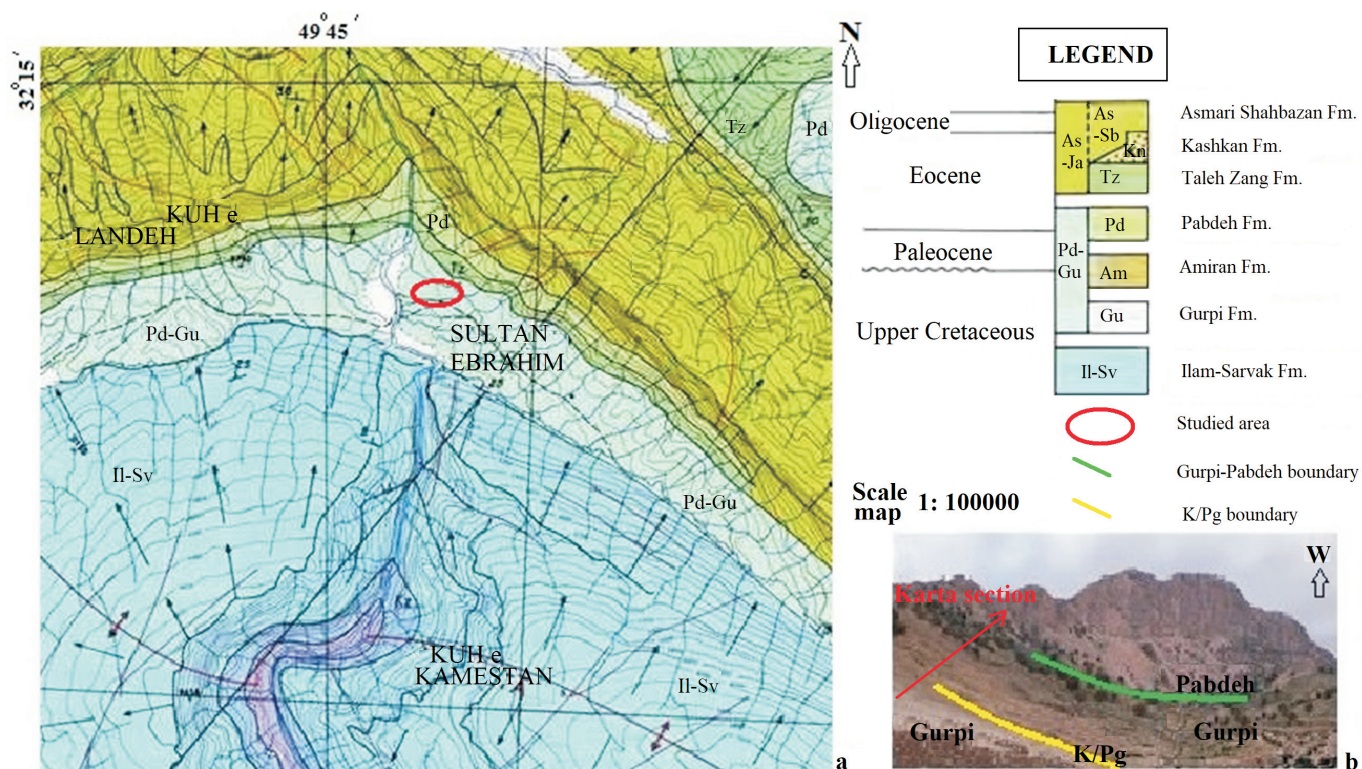
## GEOLOGICAL AND STRATIGRAPHICAL SETTING

The ca. 2000-km-long Zagros Belt is part of the Alpine-Himalayas orogenic belt with a northwest-southeast trend in Iran (Alavi 2004). The Izeh zone is a part of the Zagros belt along a southwestern fault in the Zagros highlands (Motiei 2003; Alavi 2004). This fault divides the Izeh zone into the northwestern and southeastern regions (Sherhati and Letouzey 2004; Navabpour et al. 2010), where the Bangestan Group (i.e.,

Kazhdumi, Sarvak, Surgah and Ilam Fms. in the Zagros) is well developed in the northwest area of the Izeh zone.

The Upper Cretaceous to Paleogene deposits in this area are represented by the Gurpi and Pabdeh formations. The Gurpi formation is an expanded part of the source rocks in the Zagros Basin (Motiei 1995; Kamali et al. 2006) and forms a segment of a mega-sequence spanning upper Turonian to Eocene (Ziegler 2001; Alavi 2004). The Gurpi formation consists of argillaceous limestone, marl, and pelagic shales, which form part of the sedimentary sequence in the southwest of Iran (Motiei 2003; Alavi 2004; Hemmati-Nasab et al. 2008; Beiranvand et al. 2014). The type section of the Gurpi Fm., located in Tang-e Pabdeh near Lali city, is about 320 m thick and consists of limey, gray shales. The Pabdeh formation in its type section is composed of shale and thin-bedded clay-limestone with a thickness of more than





TEXT-FIGURE 2

(a) Geological map of the Kamestan anticline showing the studied section. (b) The locations of the Gurpi and Pabdeh formations and K/Pg boundary, view to the west.

798 m. The lithostratigraphic and biostratigraphic data of these formations have been previously investigated (i.e., James and Wynd 1965; Bahrami 2009; Beiranvand and Ghasemi-Nejad 2013; Ahifar et al. 2015; Foroughi and Aryanasab 2018). The boundary between the Gurpi and Pabdeh Fms. shows no abrupt lithological changes.

The Karta section (geographical coordinates of the base: 32°12'59" N and 49° 46'50" E) is located in the anticline of Kamestan, north of Karta village, and approximately 32 km northwest of Izeh in the Khuzestan Province (Iran) and is accessible via the Izeh road to Shahid-Abbaspour Dam. This section is located on the eastern side of the dam (text-figs. 1 and 2), which consists of the Upper Cretaceous and lower Paleocene sequence including Gurpi and Pabdeh formations. The upper part of Gurpi formation consists of deep marine marl, argillaceous limestone, and gray shale with a thickness of 100.1 m. Subsequently, the lowest part of the Pabdeh formation is characterized by purple shale overlain by green shale and has a thickness of 39 m (text-fig. 3). Therefore, the upper part of the Gurpi Fm. and lowest part of the Pabdeh formation at the Karta section is 139.1 m thick. The K/Pg boundary is placed at ca. 30.4 m below the Pabdeh formation (at 69.7 m).

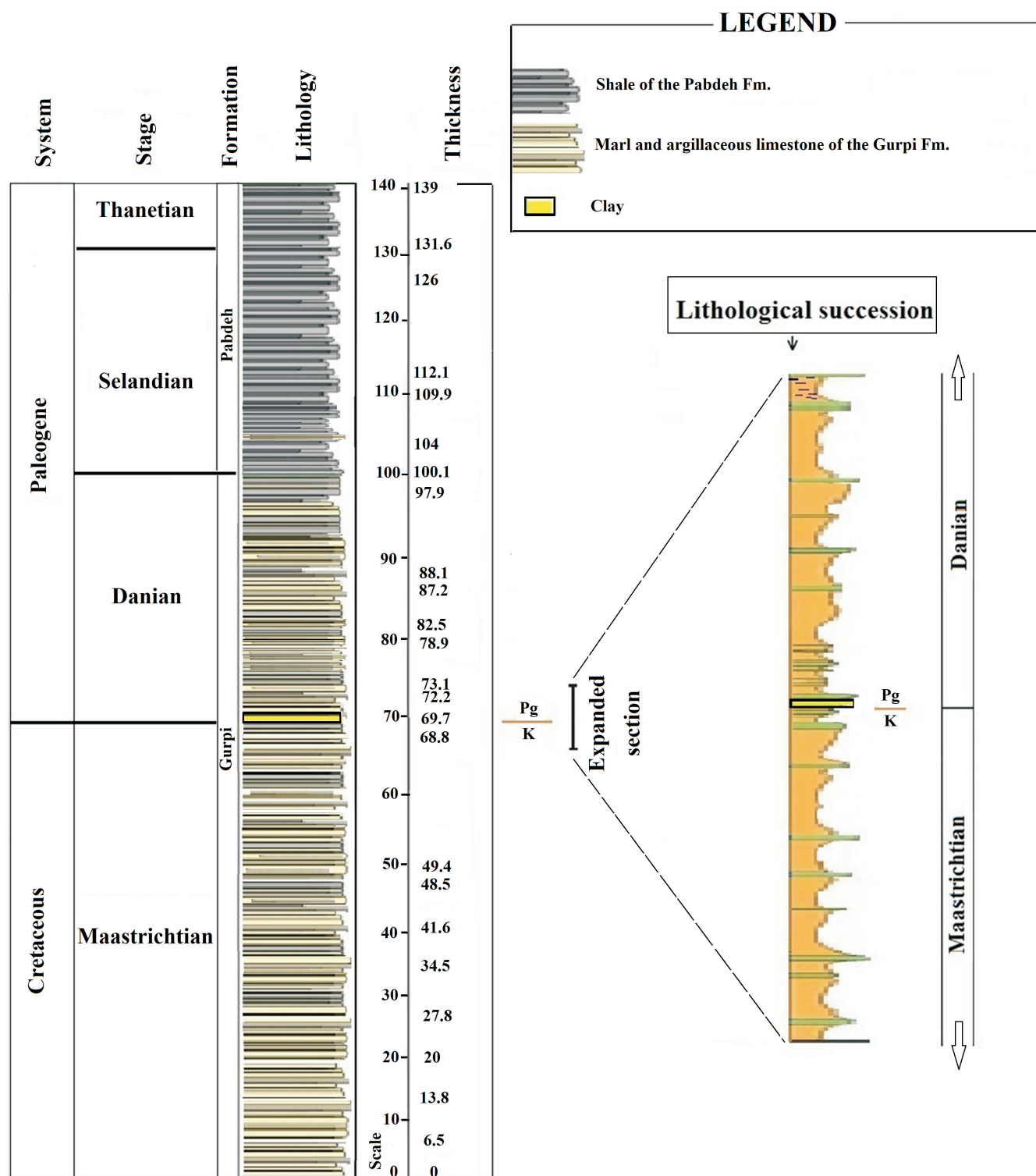
## MATERIALS AND METHODS

A total of 122 samples were collected from the upper part of Gurpi formation (89 samples: no. 1–89) and the lower part of Pabdeh formation (33 samples: no. 90–122) in the Karta section. All samples were processed for calcareous nannofossils

following the standard smear slide method of Bown and Young (1998). Smear-slides provide a rapid and simple method for the identification of calcareous nannofossils. All slides were studied under crossed polarized light (XPL) and plain polarized light (PPL) with an Olympus microscope at ×1000 magnification. For each slide, approximately 100 fields of view (FOV) were counted to identify species and the First Occurrence (FO) and Last Occurrence (LO) of taxa. Species abundances are denoted by R = rare (1 specimen per 11–100 FOV), F = few (1 specimen per 2–10 FOV), C = common (1–10 specimens per FOV), and A = abundant (>10 specimens per FOV) (Balestra et al. 2019). The preservation of calcareous nannofossils was qualitatively evaluated by considering the degree of etching (E) and overgrowth (O) (Roth 1978; Watkins 2007). Calcareous nannofossil nomenclature follows the taxonomy of Perch-Nielsen (1985a, b). For biostratigraphic analysis, the references of Martini (1971), Sissingh (1977), Burnett (1998), and Agnini et al. (2014) were followed. In this research, all the rows of samples are shown in the tables (it is clear from the continuity of the species expansion lines), only in the sample number column, several numbers of samples (from the numbers of samples) are shown that belong to the rows, which show the boundary of the zones.

## RESULTS

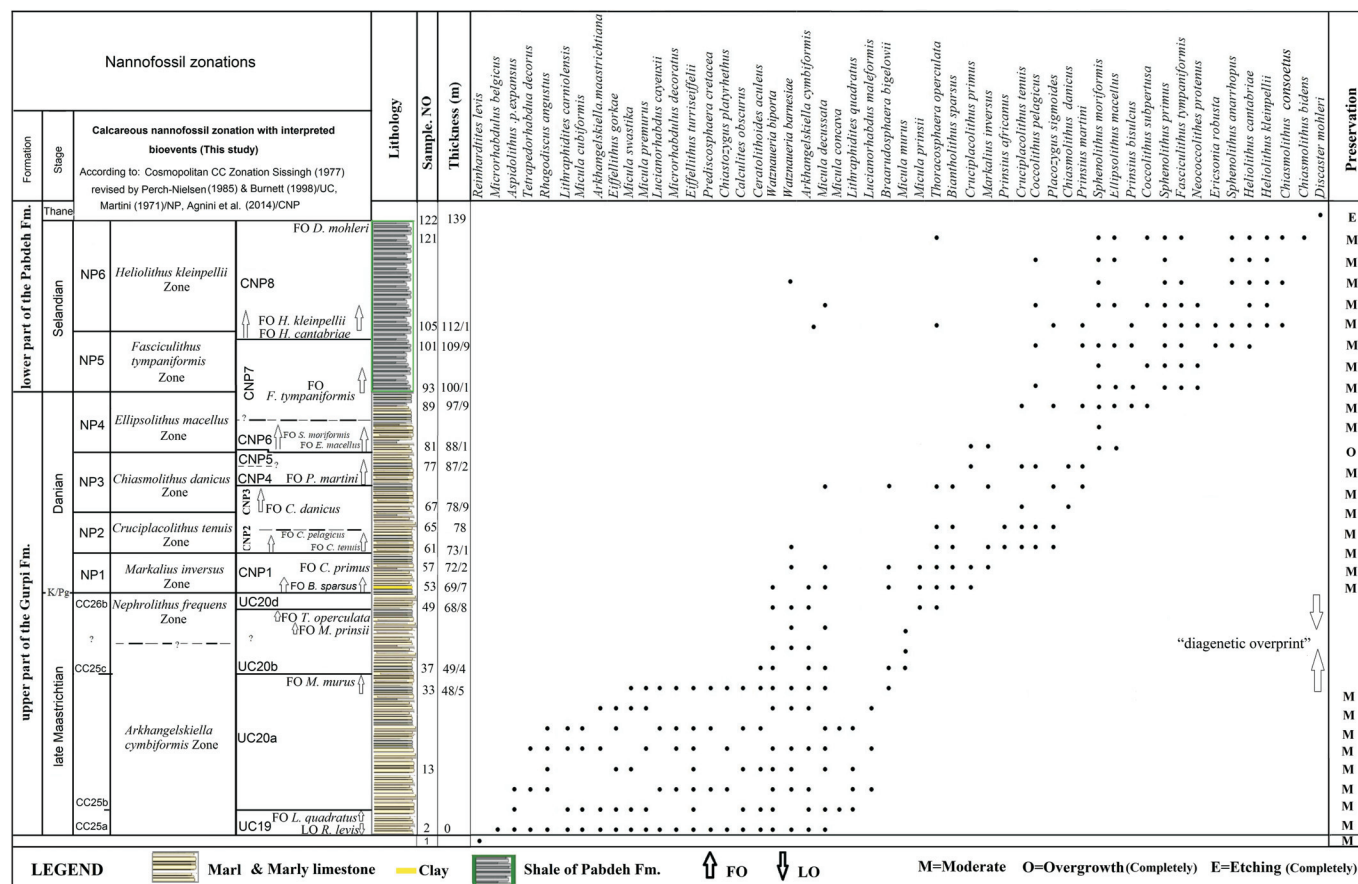
Thirty-one genera and 52 species of calcareous nannofossils are identified in the Karta section (text-figs. 4, 5). All samples contain calcareous nannofossils with a moderate (M) state of preservation that sometimes hampers their identification. Some marker species are illustrated in text-figure 5.



TEXT-FIGURE 3

Lithostratigraphy, lithology and location of samples from the Maastrichtian to Thanetian interval in the upper part of the Gurpi Fm., and lower part of the Pabdeh Fm., in the Karta section, northwest of Izeh, SW Iran.





TEXT-FIGURE 4

Lithostratigraphy, location of samples, bio-events, and nannofossil distribution for the Maastrichtian to Thanetian interval for the upper part of the Gurpi Fm., and lower part of the Pabdeh Fm., in the Karta section, northwest of Izeh, SW Iran.

## Biostratigraphy

The following main biostratigraphic events (bioevents) have been identified and correlated with the calcareous nannofossil biozones (from base to top): (1) LO of *Reinhardtites levis* at the base of the section, the base of CC25a subzone (sample 1); (2) the base of CC25b subzone is based on the FO of *Lithraphidites quadratus* at 6.5 m (sample 6); (3) the base of CC25c subzone is based on the FO of *Micula murus* at 49.4 m (sample 34); (4) FO of *Micula prinsii* at 67 m (sample 48); (5) the base of UC20d subzone is based on the FO of *Thoracosphaera operculata* at 68.8 m (sample 49); (6, 7) the base of Zone NP1 is based on the FO of *Biantholithus sparsus* and *Cruciplacolithus primus* at 69.7 m (sample 50); (8, 9) the base of Zone NP2 is based on the FO of *Cruciplacolithus tenuis* and *Coccolithus pelagicus* at 73.1 m (sample 58); (10) the base of Zone NP3 is based on the FO of *Chiasmolithus danicus* at 78.9 m (sample 66); (11) the base of Zone CNP4 is based on the FO of *Prinsius martinii* at 82.5 m (sample 72); (12) the base of Zone NP4 is based on the FO of *Ellipsolithus macellus* at 88.1 m (sample 78); FO of *Prinsius bisulcus* 94 m (sample 84) (13) the base of Zone NP5 is based on the FO of *Fasciculithus tympaniformis* at ca. 100.1 m (sample 90); (14) FO of *Sphenolithus moriformis* at 104 m (sample 95); (15) the top of Zone CNP7 is based on the FO of *Heliolithus cantabrigiae* at 112.1 m (sample 102); (16) the base of Zone NP6 is based on the FO of *Heliolithus kleinpellii* at 114

m (sample 104); (17) the top of Zone CNP8 is based on the FO of *Discoaster mohleri* at 139 m (sample 122) (text-fig. 4).

The abundances of calcareous nannofossils from the studied section (text-fig. 6) and abundances of selected nannofossils across the K/Pg boundary (text-fig. 7) are also presented. On the basis of the identified bioevents and biozones, the study section spans from the nannofossil subzone CC25a of Sissingh (1977) and Zone UC19<sup>TP</sup> of Burnett (1998) to the uppermost part to NP6 of Martini (1971) and CNP8 of Agnini et al. (2014) (text-fig. 4). Specifically, the upper part of the Gurpi Fm. covers from the late Maastrichtian (CC25a subzone of Sissingh (1977) and Zone UC19<sup>TP</sup> of Burnett (1998)) to late Danian (NP4 Zone of Martini (1971) and the middle part of Zone CNP7 of Agnini et al. (2014)). The lower part of the Pabdeh Fm. encompasses the Selandian to Thanetian interval and Zones NP5 to NP7 and middle CNP7 to the lower part of CNP9. The FOs of *L. quadratus*, *M. murus*, *T. operculata*, and of *B. sparsus* and *C. primus* mark the boundary between UC19<sup>TP</sup>/UC20a<sup>TP</sup> (CC25a/CC25b), UC20a<sup>TP</sup>/UC20b<sup>TP</sup> (CC25b/CC25c), UC20c<sup>TP</sup>/UC20d<sup>TP</sup> (CC26a?/CC26b), UC20d<sup>TP</sup>/CNP1 (CC26b/NP1), respectively (text-fig. 4).

Calcareous nannofossil bioevents from the uppermost Maastrichtian to lower Thanetian of the Karta section have led to the

# TEXT-FIGURE 5

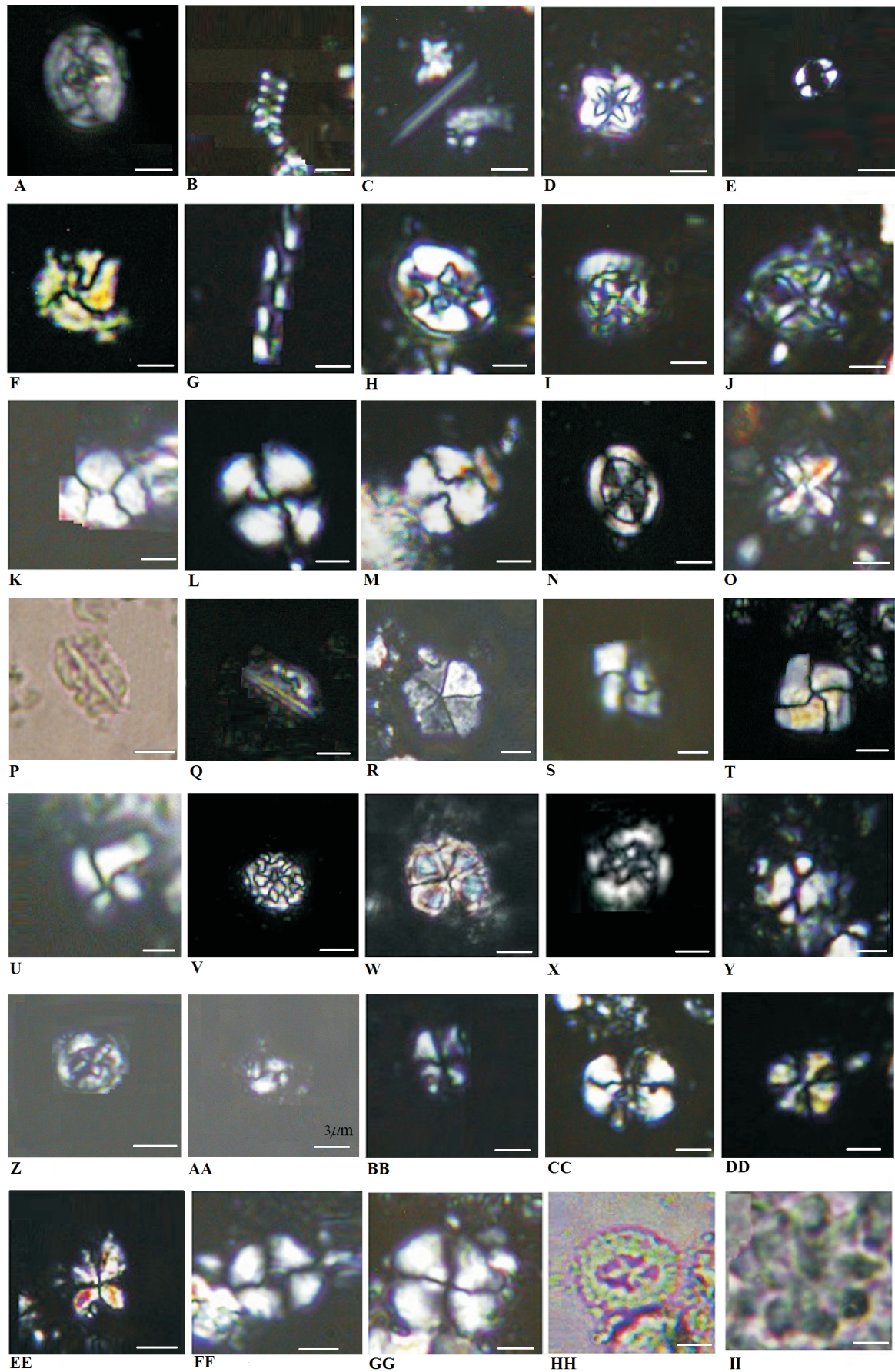
Selected nannofossil taxa found in the upper Maastrichtian to Paleocene Gurpi-Pabdeh formations.

All illustrations (XPL-PPL) light micrographs  $\times 1000$  magnification;

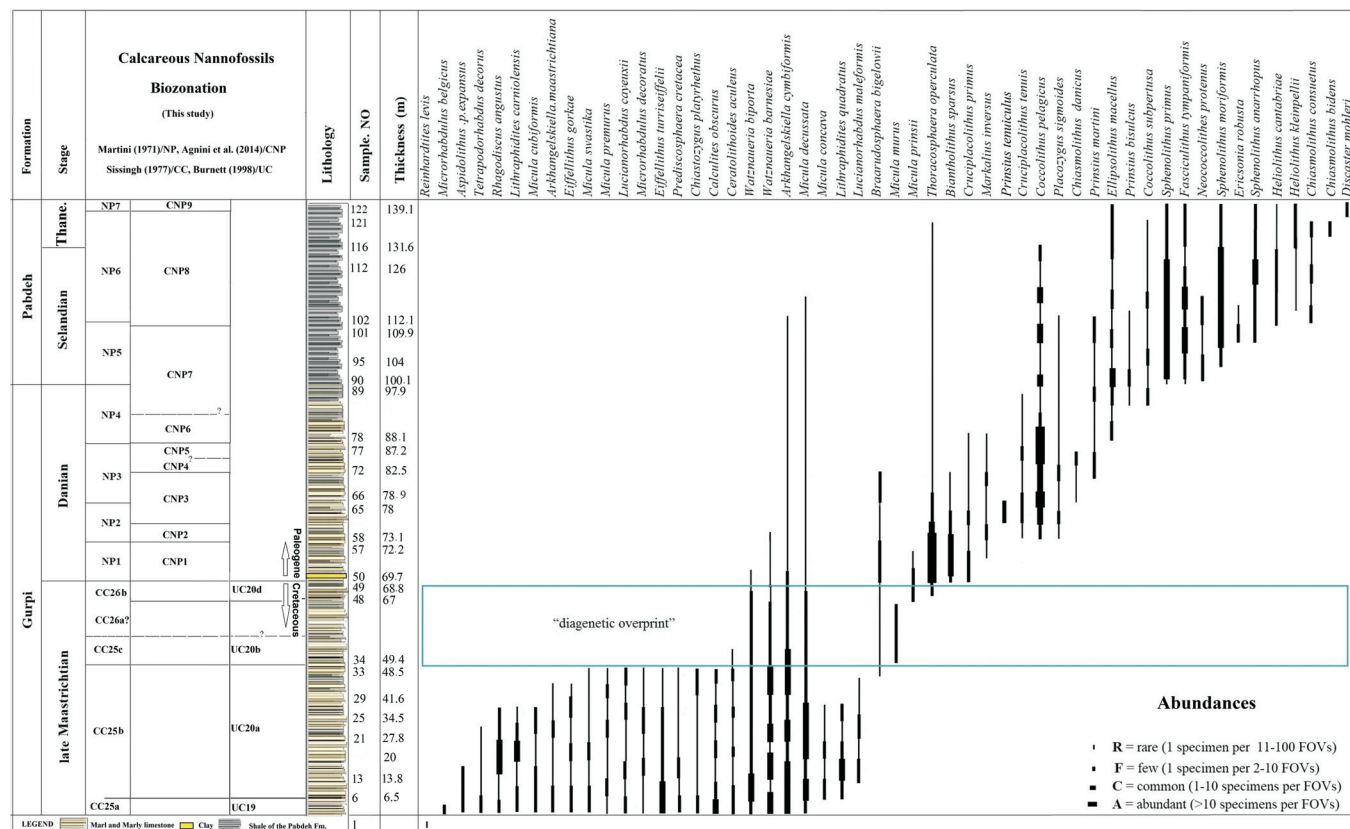
Scale bar: 5  $\mu\text{m}$ , the taxa are referenced in Perch-Nielsen (1985).

- |  |   |
|--|---|
| <p>A <i>Reinhardtites levis</i> Prins and Sissingh in Sissingh 1977, XPL (sample no. 1, the base of the section);</p> <p>B <i>Tetrapodorhabdus decorus</i> (Deflandre in Deflandre and Fert 1954) Wind and Wise 1983, XPL (sample no. 6, 6.5 m);</p> <p>C <i>Lithraphidites carniolensis</i> Deflandre 1963, XPL (sample no. 21, 27.8 m);</p> <p>D <i>Micula cubiformis</i> Forchheimer (1972), XPL (sample no. 13, 13.8 m);</p> <p>E <i>Eiffellithus gorkae</i> Reinhardt (1965), XPL (sample no. 29, 41.6 m);</p> <p>F <i>Micula swastica</i> Stradner and Steinmetz (1984), XPL (sample no. 13, 13.8 m);</p> <p>G <i>Microrhabdulus decoratus</i> Deflandre 1959, XPL (sample no. 25, 34.5 m);</p> <p>H <i>Eiffellithus turriseiffelii</i> (Deflandre in Deflandre and Fert 1954) Reinhardt (1965), XPL (sample no. 13, 13.8 m);</p> <p>I <i>Prediscosphaera cretacea</i> (Arkhangelsky 1912) Gartner 1968, XPL (sample no. 21, 27.8 m);</p> <p>J <i>Chiastozygus platyrhethus</i> Hill (1976), XPL (sample no. 33, 48.5 m);</p> <p>K <i>Calculites obscurus</i> (Deflandre 1959) Prins and Sissingh in Sissingh (1977), XPL (sample no. 29, 41.6 m);</p> <p>L <i>Watznaueria barnesiae</i> (Black in Black and Barnes 1959) Perch-Nielsen (1968), XPL (sample no. 33, 48.5 m);</p> <p>M <i>Watznaueria biporta</i> Bukry 1969, XPL (sample no. 29, 41.6 m);</p> <p>N <i>Arkhangelskiella cymbiformis</i> Vekshina 1959, XPL (sample no. 50, 69.7 m);</p> <p>O <i>Micula decussata</i> Vekshina (1959), XPL (sample no. 21, 27.8 m);</p> <p>P-Q <i>Lithraphidites quadratus</i> Bramlette and Martini 1964, PPL-XPL (sample no. 25, 34.5 m);</p> <p>R <i>Braarudosphaera bigelowii</i> (Gran and Braarud 1935) Deflandre 1947, XPL (sample no. 57, 72.2 m);</p> | <p>S <i>Micula murus</i> (Martini 1961) Bukry 1973, XPL (sample no. 35, 51.2 m);</p> <p>T <i>Micula murus</i> (Martini 1961) Bukry 1973, XPL (sample no. 34, 49.4 m);</p> <p>U <i>Micula prinsii</i> Perch-Nielsen 1979, XPL (sample no. 50, 69.7 m);</p> <p>V <i>Thoracosphaera operculata</i> Bramlette and Martini (1964), XPL (sample no. 58, 73.1 m);</p> <p>W <i>Biantholithus sparsus</i> Bramlette and Martini 1964, XPL (sample no. 58, 73.1 m);</p> <p>X <i>Cruciplacolithus tenuis</i> (Stradner 1961) Hay and Mohler in Hay et al. 1967, XPL (sample no. 66, 78.9 m);</p> <p>Y <i>Coccolithus pelagicus</i> (Wallich 1877) Schiller 1930, XPL (sample no. 78, 88.1 m);</p> <p>Z <i>Chiasmolithus danicus</i> (Brotzen 1959) Hay and Mohler 1967, XPL (sample no. 77, 87.2 m);</p> <p>AA <i>Prinsius martinii</i> (Perch-Nielsen 1969) Haq 1971, XPL (sample no. 101, 109.9 m);</p> <p>BB <i>Sphenolithus moriformis</i> (Brönnimann and Stradner 1960) Bramlette and Wilcoxon 1967, XPL (sample no. 116, 131.6 m);</p> <p>CC <i>Ellipsolithus macellus</i> (Bramlette and Sullivan 1961) Sullivan (1964), XPL (sample no. 122, 139 m);</p> <p>DD <i>Sphenolithus primus</i> Perch-Nielsen (1971), XPL (sample no. 112, 126 m);</p> <p>EE <i>Sphenolithus anarrhopus</i> Bukry and Bramlette 1969, XPL (sample no. 116, 131.6 m);</p> <p>FF <i>Heliolithus cantabriae</i> Perch-Nielsen (1971), XPL (sample no. 112, 126 m);</p> <p>GG <i>Heliolithus kleinpellii</i> Sullivan 1964, XPL (sample no. 116, 131.6 m);</p> <p>HH <i>Chiasmolithus consuetus</i> (Bramlette and Sullivan 1961) Hay and Mohler 1967, PPL (sample no. 112, 126 m);</p> <p>II <i>Discoaster mohleri</i> Bramlette and Percival 1971, PPL (sample no. 122, 139 m).</p> |
|--|---|









TEXT-FIGURE 6  
Calcareous nannofossil abundances in the studied section.

identification of nine biozones (text-fig. 4) which are presented here from base to top as follows:

#### Nannofossil Zones CC25/UC19<sup>TP</sup>-UC20a<sup>TP</sup>

This biostratigraphic interval covers from the LO of *R. levis* to the FO of *Nephrolithus frequens* and corresponds to the late Maastrichtian (Perch-Nielsen 1985; Burnett 1998). *Nephrolithus frequens* was not recorded in this studied interval, therefore, other taxa were used to approximate the upper boundary of this zone. At low latitudes, the CC25 zone is defined by the LO of *R. levis* to the FO of *N. frequens* (Perch-Nielsen 1985). The CC25a (UC19) is a subzone and was defined as the interval from the LO of *R. levis* to the FO of *L. quadratus* (at 6.5 m, sample 6), which marks the base of CC25b subzone (UC20a<sup>TP</sup>). The first occurrence of *M. murus* (49.4 m, sample 34) marks the base of Zone CC25c (text-fig. 5). Therefore, the upper limit of this biozone was defined by the FO of *M. murus*. Zones UC19<sup>TP</sup> (CC25a) and UC20a<sup>TP</sup> (CC25b) include the interval from the LO of *R. levis* to the FO of *L. quadratus* (= UC19<sup>TP</sup>), and then the FO of *L. quadratus* to the FO of *M. murus* (= UC20a<sup>TP</sup> subzone), respectively (text-fig. 4). These biozones (CC25a and CC25b) cover 49.4 m of the Gurpi Formation and consist of marls and shales.

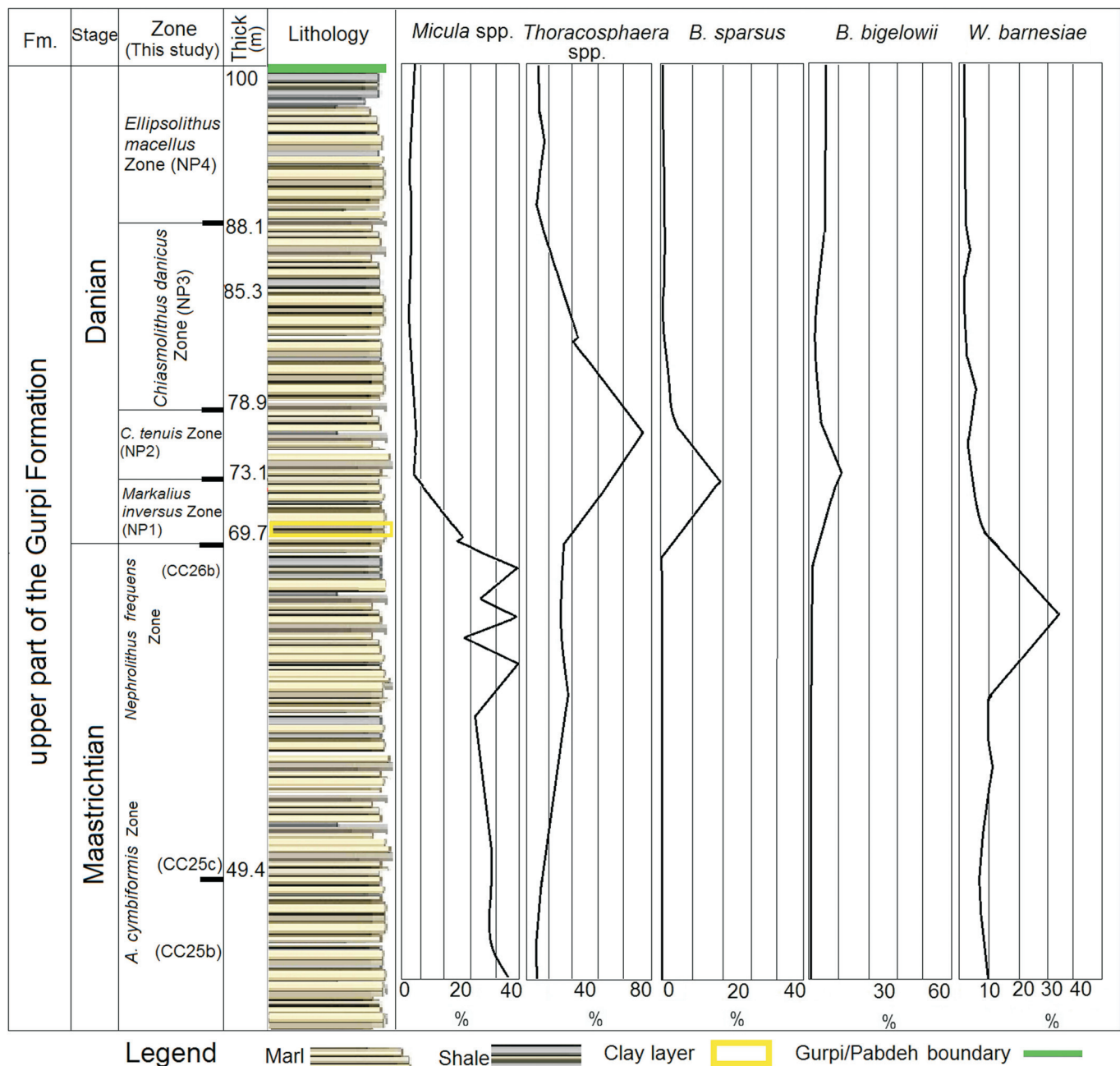
#### Nannofossil Zones CC26b/UC20b<sup>TP</sup>-UC20d<sup>TP</sup>

According to Perch-Nielsen (1985), the CC26 Zone is defined as the biostratigraphic interval from the FO to LO of *N. frequens*. This zone corresponds to the latest Maastrichtian. As

mentioned above, the *N. frequens* was not recorded in the studied section, hence, it was not possible to define the lower and upper boundary of CC26 zone. Here, the FO of *Ceratolithoides kamptneri* is not recorded at the upper part of UC20b<sup>TP</sup>. Accordingly, the UC20b<sup>TP</sup>/UC20c<sup>TP</sup> boundary is not recognizable. The absence of *C. kamptneri* might be potentially ascribed to low sampling resolution. The subzone CC26b is equivalent to UC20d<sup>TP</sup> of Burnett (1998) and, the FO of *M. prinsii* marks the base of UC20d<sup>TP</sup>. The data obtained from the biostratigraphic analysis of the Karta section indicate that CC26 zone is incomplete; so that, both *N. frequens* and *Ceratolithoides kamptneri* were not identified here. The FO of *M. prinsii*, which marks the base of CC26b subzone, occurs at 67 m in sample 48 (text-figs. 4, 6). The bloom of *Thoracosphaera* at the beginning of the Paleocene together with *M. prinsii* might suggest the beginning of warm conditions in the Paleocene. This subzone (CC26b) with a thickness of about 2.7 m is characterized by the occurrence of marls and shales of the upper part of the Gurpi formation (text-fig. 4).

#### Nannofossil Zones NP1/CNP1

The first calcareous nannofossil zone recorded in the lowermost Paleocene is the *Markalius inversus* Zone (Martini 1971) that is early Danian in age (Perch-Nielsen 1985). This zone extends from the last occurrence of Cretaceous taxa to FO *C. tenuis* (Martini 1971). In this study, Zone NP1 is defined as the interval between the FO of *B. sparsus* (as in Perch-Nielsen 1979 in the North Sea) and the FO of *C. tenuis* and represented by sam-



TEXT-FIGURE 7

Abundance curves for selected calcareous nannofossils across the K/Pg transition and detailed lithological succession of the studied section. The yellow rectangle shows the clay layer on the K/Pg boundary.

ples 50–57 (text-figs. 4, 6). The NP1 zone is also characterized by the FO of the species *C. primus* at 69.7 m (sample 50), *M. inversus* (71.8 m, sample 55) and *B. sparsus* (69.7 m, sample 50). In this study, *Markalius inversus* is a rare species. The predominant taxa of this interval are *Thoracosphaera* spp., *B. sparsus*, *C. primus* and *B. bigelowii* (text-figs. 5, 7); Cretaceous species are present but rare. This zone is equivalent to CNP1 zone of Agnini et al. (2014). The FO of *C. pelagicus* defines the top of CNP1 or the boundary of CNP1/CNP2 zones (Agnini et al. 2014). At this section, Zone NP1 consists of 3.4 m of marl in

the upper part of the Gurpi formation; the base of this zone coincides with the K/Pg boundary.

#### Nannofossil Zones NP2/CNP2- (lower) CNP3

The *Cruciplacolithus tenuis* Zone (NP2) is the interval from the FO of *C. tenuis* to the FO of *C. danicus* Martini (1971) zonation and corresponds to the early Danian. This zone is equivalent to Zone CNP2 and the lower part of Zone CNP3 of Agnini et al. (2014). The FO of *C. pelagicus* marks the base of CNP2 in this study, this event is found at 73.1 m level (sample 58). Also, the

FO of *Praeprinsius dimorphosus* defines the top of CNP2 (Agnini et al. 2014). However, we recorded the species *P. tenuiculus*, which is part of the *Praeprinsius dimorphosus* group, at the base of the CNP3 zone or top CNP2, which is also common in terms of abundance. Therefore, the top of CNP2 or the CNP2/ CNP3 boundary at 75 m level (sample 61) has been determined. Zone NP2 covers a 5.8 m-thick-interval of marls in the upper part of the Gurpi Fm. (text-figs. 4, 6, 7).

#### Nannofossil Zones NP3/ (upper) CNP3–CNP4

The *Chiasmolithus danicus* Zone (NP3) is defined as the interval from the FO of *C. danicus* to the FO of *E. macellus* (Martini 1971) and corresponds to the middle-late Danian age. It is equivalent to the upper part of Zone CNP3 and the lower part of CNP4 of Agnini et al. (2014). The FO of *C. danicus* occurs at 78.9 m (sample 66) (text-figs. 4, 6). The FO of *P. martini* at 82.5 m (sample 72) marks the CNP3/CNP4 boundary that falls in the Gurpi Fm. Zone NP3 consists of 9.2 m of marls in the upper part of the Gurpi Fm.

#### Nannofossil Zones NP4/CNP6–CNP7

The NP4 Zone is defined from the FO of *E. macellus* to the FO of *F. tympaniformis* (Martini 1971), which belongs to the late Danian. The *Ellipsolithus macellus* Zone encompasses the uppermost part of the Gurpi Fm. at the Karta section and is represented by samples 78–89 (text-figs. 4 and 6). Zone NP4 is defined from the FO of *E. macellus* to the FO of *F. tympaniformis* (Martini 1971) and is of late Danian age. Also, in this study, the FO of *Prinsius bisulcus* (94 m, sample 84) is recorded in the upper part of NP4 zone (text-fig. 4). Zone NP4 from Martini (1971) is equivalent to CNP6 and the lower part of CNP7 from the Agnini et al. (2014) zonation. In this study, the base of NP4/CNP6 (Agnini et al. 2014) is placed at the FO of *E. macellus* at 88.1 m (sample 78), and the top of the NP4 Zone is defined by the FO of *F. tympaniformis* (100.1 m, sample 90). Furthermore, as the FO of *Toweius pertusus* and *Fasciculithus ulii* were not recorded, the boundaries of CNP4/CNP5 (upper part of NP3) and CNP6/CNP7 (in the middle part of NP4) zones have not been determined. The NP4 zone covers ca. 12 m of marls and shales in the upper part of the Gurpi Fm. Our investigation suggests that the uppermost part of the Gurpi Fm. is latest Danian in age. Close to the Danian/Selandian boundary, there was a change in lithology and the Gurpi Fm. is gradually replaced by the pelagic shale of the Pabdeh Fm.

#### Nannofossil Zones NP5/ (upper) CNP7- (lower) CNP8

The NP5 Zone is defined from the FO of *F. tympaniformis* to the FO of *Heliolithus kleinpellii* (Martini 1971). This zone corresponds to Selandian. The lower part of the Pabdeh Fm. falls within the *Fasciculithus tympaniformis* Zone (NP5) of Martini (1971). Zone NP5 is defined as the interval from the FO of *F. tympaniformis* (100.1 m, sample 90) to the FO of *H. kleinpellii* (114 m, sample 104) and is ascribed to the Selandian (text-fig. 4). NP5 correlates with the upper part of Zone CNP7 and the lowermost part of CNP8 (Agnini et al. 2014). The FO of *H. cantabriae* defines the top of CNP7 (Agnini et al. 2014) and is placed at 112.1 m (sample 102) from the base of the section. The thickness of Zone NP5 is ca. 12 m.

#### Nannofossil Zones NP6/ (upper) CNP8

Zone NP6 is defined from FO of *H. kleinpellii* to FO of *Discoaster mohleri* (Martini 1971), which corresponds to the Selandian–Thanetian transition. Zone NP6 is equivalent to the upper part of Zone CNP8 (Agnini et al. 2014) and is represented

by samples 102–121 (text-figs. 4, 6). NP6 is characterized by nannofossil assemblages including *H. cantabriae*, *H. kleinpellii*, *F. tympaniformis*, *C. pelagicus*, *S. primus*, *S. moriformis*, *Sphenolithus anarrhopus* among others (text-figs. 4, 5, 6). The FO of *D. mohleri* at 139 m depth (sample 122) indicates the top CNP8. The NP6 interval falling includes approximately 27 m of grey and green shales in the lower part of the Pabdeh Fm.

#### Nannofossil Zones NP7 (lower)/ CNP9

The NP7 zone is defined from FO of *Discoaster mohleri* to FO of *Heliolithus riedelii* and/or *Discoaster nobilis* (Martini 1971). In this study, FO of *H. riedelii* and *D. nobilis* were not recorded. The presence of *D. mohleri* defines the base of Zone NP7 (Martini 1971) and is equivalent to the lower part of Zone CNP9 of Agnini et al. (2014) (text-fig. 4). Zone CNP9 is defined as the interval from the FO of *D. mohleri* to the FO of *Discoaster backmanii* and is ascribed to the Thanetian. In this study, FO of *D. mohleri* (139 m, sample 122) at the lower part of CNP9 zone (lower part of NP7) or CNP8/CNP9 boundary (NP6/NP7 boundary) is recorded. The FO of *D. backmanii* is not recorded, therefore, the upper part of CNP9 zone have not been determined. In Agnini et al. (2014) zonation, CNP9 forms the lower part of the NP7 zone. The lithology at the top of the studied section falling within NP7 includes grey and green shales in the lower part of the Pabdeh Formation.

## DISCUSSION

### Stage boundaries

Calcareous nannofossils represent an important component of deep-sea carbonate sediments due to their cosmopolitan distribution and high abundance in marine sediments, and have been widely used as powerful tools for dating Cretaceous and Cenozoic records (e.g. Sissingh 1977; Burnett 1998; Agnini et al. 2014; Raffi and Backman 2022) as well as for constraining stage boundaries.

On the basis of our dataset and previous findings in the area (Hemmati-Nasab et al. 2008; Bahrami 2009), the Gurpi and Pabdeh formations of the Karta section are inferred to have been deposited in open marine conditions. Our results suggest that the K/Pg boundary in the upper part of Gurpi formation is continuous and is placed at 30.4 m below the Gurpi–Pabdeh contact, within the marl and argillaceous limestone of the Gurpi formation. The occurrence of calcareous nannofossils such as *M. prinsii* and *Thoracosphaera* spp. in the late Maastrichtian (CC25 and CC26b) as well as FO of *B. sparsus* in the early Danian (NP1) support the identification and constrain the K/Pg boundary in the Karta section. Calcareous nannofossil bioevents in our study enable us to identify three stage boundaries.

### Cretaceous–Paleogene boundary (K/Pg)

In the K/Pg Global Stratigraphic Section and Point (GSSP) at El Kef (Tunisia), the boundary is characterized by LOs of Cretaceous nannofossil taxa and the FOs of Paleogene calcareous nannofossils (e.g. bloom of *Thoracosphaera* spp., *Braarudosphera*, *C. primus*), as well as decreasing values (low species richness) of calcareous nannofossils at the boundary (Keller 2004, 2011; Molina et al. 2006).

The Karta section in the Zagros Basin provides a stratigraphically continuous sequence covering the K/Pg boundary that falls between CC26b (UC20d) and NP1 (CNP1) Zones



Age	Sissingh (1977) emended by Perch-Nielsen(1985)(CC) and Martini (1971)(NP)		Burnett (1998) Cretaceous (UC) and Agnini et al. (2014)(CNP)		Egypt	Zagros, Iran			This work		Gurpi Fm. / Pabdeh Fm.
	Zones NP/CC	Events	Zones CNP/UC	Events	Khalil and Zahran (2014) (Sinai)	Razmjooei et al. (2018) (Fars)	Senemari (2018) Bulfars section (Dezful em./Izeh)	Senemari (2017) Kalchenar section (Izeh)	Sissingh (1977) /Cretaceous(CC) and Martini (1971)(NP) (Iran Izeh) *continued	Burnett (1998) /Cretaceous(UC) and Agnini et al. (2014) /Paleocene(CNP)	
Thanetian	NP7	▲ <i>D. mohleri</i>	CNP9						NP7	▲ <i>D. mohleri</i>	CNP9
Selandian	NP6	▲ <i>H. kleinpellii</i>	CNP8	▲ <i>H. kleinpellii</i>	Hiatus	Hiatus	NP6	NP6	NP6	▲ <i>H. kleinpellii</i>	CNP8
	NP5	▲ <i>F. tympaniformis</i>	CNP7	▲ <i>F. cantabrigiae</i>	NP5	NP5	NP5	NP5	NP5	▲ <i>F. tympaniformis</i>	CNP7
Danian	NP4	▲ <i>E. macellus</i>	CNP6	▲ <i>F. ulii</i>	NP4		Hiatus	NP4	NP4		CNP6
			CNP5	▲ <i>Ch. bidens</i>		NP3		NP3	NP3		CNP5
			CNP4	▲ <i>P. martini</i>	NP3			NP2	NP2		CNP4
	NP3	▲ <i>Ch. danicus</i>	CNP3	▲ <i>Ch. danicus</i>	Hiatus			NP1	NP1		CNP3
	NP2	▲ <i>Cr. tenuis</i>	CNP2	▲ <i>C. pelagicus</i>	Hiatus			NP1	NP1		CNP2
	NP1		CNP1	▲ <i>Cr. primus</i>	Hiatus			NP1	NP1		CNP1
Upper Maastrichtian	CC26	▼ <i>N. frequens</i>	UC20d	▼ <i>M. prinsii</i>	Hiatus	CC26b	UC20d	CC26b	UC20d	▼ <i>N. frequens</i>	UC20d
	a	▲ <i>M. prinsii</i>	UC20e	▲ <i>C. kamptneri</i>		CC26a	UC20e	CC26a	UC20e	▲ <i>M. prinsii</i>	UC20b
	CC25	▼ <i>M. prinsii</i>	UC20b	▼ <i>M. prinsii</i>	CC25c	CC25c	UC20b	CC25c	UC20b	▼ <i>M. prinsii</i>	UC20a
	b	▲ <i>L. quadratus</i>	UC20a	▲ <i>L. quadratus</i>		CC25a	UC19	CC25	UC19	▲ <i>L. quadratus</i>	UC19
	a		UC19								
		▼ <i>R. levis</i>		▼ <i>R. levis</i>							
<div>Legend: First Occurrence ▲ Last Occurrence ▼</div>											

TEXT-FIGURE 8

Comparison between Late Cretaceous to early Thanetian calcareous nannofossil standard zonation schemes of the Tethyan Realm with biozonations established for the Zagros Basin and Egypt. The boundary of the Gurpi and Pabdeh formations is indicated by a red line. The dotted line represents the unconformity boundary and the continuous line indicates the continuous boundary.

(text-figs. 4 and 6). This boundary includes samples 49 and 50 and has a thickness of 9 cm. The lowermost part of Danian in the Karta section is characterized by the appearance of new Paleogene species such as *B. sparsus*, *C. primus* and then *C. pelagicus* along with bloom of *Thoracosphaera* spp. (from sample 49 onwards). These FOs and changes in species abundances (particularly of *Thoracosphaera* spp., *B. sparsus*, *B. bigelowii*) provide the basis for the identification of the lowermost Danian NP1 (CNP1) and NP2 zones (CNP2 and lower part of CNP3) (text-figs. 6 and 7). In this lower Danian sequence, sediments contain rare Cretaceous species such as *M. prinsii*, *M. decussata* and *Watznaueria barnesiae* (text-figs. 4, 6) (Bernaola and Monechi 2007; Farouk 2014) that are considered as Cretaceous reworked specimens.

Some genera of Cretaceous nannofossil such as *Watznaueria* and *Arkhangelskiella* only sporadically occur with relatively low percentages. In fact, most of calcareous nannofossil taxa disappeared at the K/Pg boundary, and only a few calcareous nannofossil taxa of the Late Cretaceous occur in the aftermath of the K/Pg boundary (Bernaola and Monechi 2007; Farouk 2014). In this study, there is a strong decline in specimen diversity and abundance between 67–69.7 m (samples 48–50) at the K/Pg boundary, which is accompanied by bloom in *Thoracosphaera* spp. (text-figs. 4, 6, 8). Stratigraphic evidence supports that sediments such as clays are associated with a sharp drop in calcareous nannofossil assemblage in the lowermost part of the Danian (Tantawy 2003). The FOs of biostratigraphic marker species recorded within the upper Maastrichtian-lower Danian interval represent nannofossil bioevents that are commonly found in the K/Pg continuous successions of both the Tethys and Boreal realms (Senemari 2017; Vellekoop et al. 2017). The major extinction of taxa delineates a sudden change in the environmental conditions and supports the identification of the K/Pg boundary.

#### An apparent record of stepwise extinction across the K/Pg interval

The ranges of nannofossil taxa recorded in the Karta section show an apparent stepwise extinction with progressive extinctions recorded in UC20a<sup>TP</sup> (CC25b; depth range 48.5 m), a sharp extinction-level recorded at the base of UC20b<sup>TP</sup> (CC25c; depth range 49.4 m, text-fig. 5), and another gradual extinction of Cretaceous nannofossils in the lowermost Danian (samples 50; depth range 69.7 m). These features are unlikely to reflect a stable and constant extinction pattern, as it contradicts the findings in numerous records around the world (e.g. Jiang and Gartner 1986; Pospichal 1996; Keller 2004; Coccioni et al. 2010). In particular, extinctions are not generally recorded in the late Maastrichtian, except in the Central Pacific, where species richness decrease during UC20d<sup>TP</sup> (CC26b) but increase again and fully recover just before the K/Pg boundary (Thibault and Gardin 2010). Given the generally moderate preservation observed in our samples (text-fig. 4), along with low species richness (variety/in the diagenetic overprint range; text-fig. 6; samples 33–49) compared with below and above the K/Pg boundary, it is possible that extinction patterns reflect a preservation bias (text-fig. 6) (Keller 2004; Coccioni et al. 2010). Hence, the Karta section might represent a perfect example of the Signor-Lipps theoretical effect that appears to be very much enhanced by diagenesis.

#### Danian/Selandian boundary

The Danian/Selandian boundary and GSSP have been largely investigated (Guasti et al. 2006; Bernaola et al. 2006; Farouk and Faris 2012; Khalil and Al Sawy 2014). In the Karta section, the Danian/Selandian boundary corresponds to the lowermost part of NP5 (upper part of CNP7) and, in fact, follows the second radiation of *Fasciculithus*. Indeed, the Danian/Selandian boundary is approximated by the FO of *F. tympaniformis* (Agnini et al. 2014). The first radiation of *Fasciculithus* by FO *Fasciculithus ulii* occurred in the middle of the NP4 zone (Agnini et al. 2014). In the

absence of the identification of the second radiation of the *Fasciculithus* (i.e. *F. billii*, *F. janii*, *F. involutus*, and *F. pileatus*), the FO of *F. tympaniformis* is here used to approximate the Danian/Selandian boundary that is set at the lowest part of NP5 and close to the boundary of the Gurpi and Pabdeh formations. (text-figs. 4, 6).

#### Selandian/Thanetian boundary

The Selandian/Thanetian boundary is coincident with the base of magnetic polarity chron C26n (Schmitz et al. 2011) and the Early Late Paleocene Event (ELPE), also known as the Mid-Paleocene Biotic Event (MPBE). In this study, the Selandian/Thanetian boundary was identified based on the abundance of *H. kleinpellii* species (few abundance) (text-fig. 6). This is comparable to Agnini et al. (2014). Some researchers have also inferred the beginning of ELPE by changes in the relative abundance of *H. cantabriae* and *H. kleinpellii* (Coccioni et al. 2019). As no palaeomagnetic data are available for the Karta section, here the change in abundance of the two species *H. cantabriae* and *H. kleinpellii* is used to define the base of the Thanetian (131.6 m and sample 116) (text-fig. 6).

#### Correlation with some other Neo-Tethyan stratigraphic records

The results of our study in the Karta section can be compared with sections in Egypt (Khalil and Zahran 2014), Zagros Basin (Senemari 2017, 2018; Razmjooei et al. 2018), and with the standard nannofossil zonations of the Late Cretaceous of Sissingh (1977), Perch-Nielsen (1985), and Burnett (1998), and those of the Paleocene of Martini (1971) and Agnini et al. (2014) for the Tethyan Realm (text-fig. 7).

The Gurpi formation spans the interval from the upper Maastrichtian to the upper Paleocene in the different regions of the Zagros Basin (Alavi 2004). In the Karta section, subzone CC26a (UC20c) is not recorded in the upper part of the Gurpi Fm., while in some previous studies for example Razmjooei et al. (2018) (e.g. in Fars Province), a continuous record is observed from subzones CC25c through CC26a. Senemari (2017, 2018) recorded an unconformity in the upper Maastrichtian (UC20a/CC25b and UC20c/CC26a) of the Kalchenar section and the uppermost Maastrichtian (CC26/UC20d) of the Bulfars section in the Zagros Basin. In Egypt (Sinai section), Khalil and Zahran (2014) only recorded subzone CC25c (upper Maastrichtian).

The identified zones, bioevents and their correlations between other sections are shown in text-figure 8. Regarding the Paleocene, in the Karta section and also in the Kalchenar section (Senemari 2017), the Paleocene biozones appear to be continuous using the NP zonation scheme, but in the case of CNP zones, for example due to the lack of indicator species *T. pertusus*, the boundary between CNP4–CNP5 zones was not determined. However, in other locations (Khalil and Zahran 2014; Razmjooei et al. 2018; Senemari 2018/ text-fig. 7), the Paleocene sections were found to be incomplete. Variation in calcareous nannofossil assemblages in different parts of the Tethyan region may reflect a wide range of palaeo-environmental conditions (Coccioni et al. 2012; Vellekoop et al. 2017).

#### CONCLUSION

Samples were examined for calcareous nannofossils biostratigraphy from the upper part of the Gurpi and lower part of the

Pabdeh formations in the Karta section (northwest Izeh, Zagros Basin, southwestern Iran). This section appears to be stratigraphically complete and continuous across the K/Pg boundary. The calcareous nannofossil assemblages are highly abundant and are moderately well preserved, that allow us to identify biozones and to document the changes across the K/Pg boundary. In this study, nine calcareous nannofossils zones are recognized from the upper part of the Gurpi formation: *Arkhangelskiella cymbiformis* Zone (CC25a, CC25b and CC25c, late Maastrichtian), *Nephrolithus frequens* Zone (CC26b, latest Maastrichtian), *Markalius inversus* Zone (NP1, early Danian), *Cruciplacolithus tenuis* Zone (NP2, early Danian), *Chiasmolithus danicus* Zone (NP3, late Danian) and *Ellipsolithus macellus* Zone (NP4, late Danian). The *Fasciculithus tympaniformis* Zone (NP5, early Selandian), *Heliolithus kleinpellii* Zone (NP6, late Selandian–Thanetian), and *Discoaster mohleri* Zone (NP7, early Thanetian), are assigned to the lower part of the Pabdeh formation. The *Arkhangelskiella cymbiformis* Zone (CC25/ UC19, UC20a, UC20b) in the Karta section can be sub-divided into three subzones (CC25a, CC25b and CC25c) based on the ranges of *L. quadratus* (CC25a/CC25b boundary) and *M. murus* (CC25b/CC25c boundary). A minor hiatus is identified by the absence of *C. kamptneri*. In the present study, the FO of *M. prinsii* followed by the FO of *B. sparsus* and a bloom of *Thoracosphaera* spp., are used to approximate the K/Pg boundary. Therefore, based on these new data (presence of blooms of *Thoracosphaera*, *Praeprinsius* group and *Braarudosphaera*), the K/Pg boundary within the Karta section is apparently continuous and placed in the upper part of the Gurpi Fm. Above the K/Pg boundary a few centimeters of clay-enriched pelagic shale of the basal Danian (NP1 Zone) are present. Analyses of calcareous nannofossils reveal a record of abrupt extinction and species decline across the K/Pg boundary suggesting that the K/Pg boundary in the upper part of the Gurpi formation is continuous. In addition, our investigation constrains the Danian/Selandian and Selandian/Thanetian boundaries, located at the Gurpi and Pabdeh boundary and, the lower part of the Pabdeh formation, respectively. The Danian/Selandian boundary is between NP4 and NP5 and within CNP7 and is defined here based on the FO of *F. tympaniformis*. The Selandian/Thanetian boundary is located between the abundance changes of *H. cantabriae* and *H. kleinpellii* (changes in percentage of abundance of species/131.6 m, sample 116) (text-fig. 6). The correlation of the recognized biozones from the part of Izeh province sections (Bulfars, Kalchenar and this study) with the parts of the Fars and Egypt provides insights about the boundary changes of their zones (text-fig. 8).

#### ACKNOWLEDGMENTS

The authors thank Prof. N.R. Thibault and Dr. M.J. Razmjooei (Postdoctoral Researcher/ Marine Geologist at Stockholm University) for their generous support and assistance.

#### REFERENCES

- AFGHAH, M. and GHIYASI, A. A., 2013. Biostratigraphy of Gurpi Formation (late Cretaceous) in interior Fars: Bavan area, central Zagros (southwestern Iran). *Journal of Earth Science and Climatic Change*, 4: 137; <https://doi.org/10.4172/2157-7617.1000137>.
- AGNINI, C., FORNACIARI, E., RAFFI, I., CATANZARITI, R., PALIKE, H., BACKMAN, J. and RIO, D., 2014. Biozonation and biochronology of Paleogene calcareous nannofossils from low and

- middle latitudes. *Newsletters on Stratigraphy*, 7: 131–181. <https://doi.org/10.1127/0078-0421/2014/0042>.
- AHIFAR, A., KANI, A. and AMIRI BAKHTIARI, H., 2015. Calcareous nannofossil biostratigraphy of Pabdeh Formation at Gurpi anticline. *Geosciences*, 24: 107–120. <https://doi.org/10.22071/gsj.2015.42301>.
- ALAVI, M., 2004. Regional stratigraphy of the Zagros fold-thrust belt of Iran and its proforeland evolution. *American Journal of Science*, 304: 1–20. <https://doi.org/10.2475/ajs.304.1.1>.
- BABAZADEH, A., BAHARAN, S., PARVANEHNEJAD SHIRAZI, M. and BAHRAMI, M., 2009. Biostratigraphy of the Pabdeh Formation in Tang-e Zanjiran (southeast Shiraz), based on plankton Foraminifera. *Stratigraphy and Sedimentology Research*, 26: 145–158; (in Persian, with English abstract).
- BAHRAMI, M., 2009. Microfacies and sedimentary environments of Gurpi and Pabdeh formations in southwest of Iran. *American Journal of Applied Science*, 6: 1295–1300. <https://doi.org/10.3844/ajassp.2009.1295.1300>.
- BALESTRA, B., VOELKER, A. and FLORES, J. A., 2019. Data report: early Pleistocene calcareous nannofossils, IODP Expedition 339, Site U1387. *Proceedings of the Integrated Ocean Drilling Program*, 339: 1–5. <https://doi.org/10.2204/iodp.proc.339.205.2019>.
- BEIRANVAND, B. and GHASEMI-NEJAD, E., 2013. High resolution planktonic foraminiferal biostratigraphy of the Gurpi Formation, K/Pg boundary of the Izeh Zone, SW Iran. *Revista Brasileira de Paleontologia*, 16: 5–26. <https://doi.org/10.4072/rbp.2013.1.01>.
- BEIRANVAND, B., GHASEMI-NEJAD, E. and KAMALI, M. R., 2013. Palynomorphs' response to sea-level fluctuations: a case study from Late Cretaceous–Paleocene, Gurpi Formation, SW Iran. *Geopersia*, 3: 11–24. <https://doi.org/10.22059/jgeope.2013.31928>.
- BEIRANVAND, B., GHASEMI-NEJAD, E., KAMALI, M. R. and AHMADI, A., 2014. Sequence stratigraphy of the late Cretaceous–Paleocene Gurpi Formation in southwest Iran. *GeoArabia*, 19: 89–102. <https://doi.org/10.2113/geoarabia190289>.
- BERNAOLA, G. and MONECHI, S., 2007. Calcareous nannofossil extinction and survivorship across the Cretaceous–Paleogene boundary at Walvis Ridge (ODP Hole 1262C, South Atlantic Ocean). *Palaeogeography, Palaeoclimatology, Palaeoecology*, 255: 132–156. <https://doi.org/10.1016/j.palaeo.2007.02.045>.
- BERNAOLA, G., BACETA, J. I., ORUE-ETXEBARRIA, X., ALEGRET, L., MARTIN-RUBIO, M. and DINARÉS TURELL, J., 2006. Calcareous nannofossil and foraminifera profiles across the Mid Paleocene biotic event at the classical Zumaia Section. In: 6th International Conference on the Climate and Biota of the Early Paleogene. Abstract, 19.
- BOWN, P. R. and YOUNG, J. R., 1998. Techniques. In: Bown, P. R., Ed., *Calcareous nannofossil Biostratigraphy*, 16–28. London: British Micropalaeontological Society Publication Series, Chapman and Hall Ltd. Kluwer Academic Publisher.
- BURNETT, J. A., 1998. Upper Cretaceous. In: Bown, P. R., Ed., *Calcareous Nannofossil Biostratigraphy*, 132–199. London: British Micropalaeontological Society Publication Series, Chapman and Hall Ltd. Kluwer Academic Publisher.
- COCCIONI, R., FRONTALINI, F., BUNCALA, G., FORNACIARI, E., JOVANE, L. and SPROVIERI, M., 2010. The Dan-C2 hyperthermal event at Gubbio (Italy): Global implications, environmental effects, and cause(s). *Earth and Planetary Science Letters*, 297: 298–305. <https://doi.org/10.1016/j.epsl.2010.06.031>.
- COCCIONI, R., BANCALA, G., CATANZARITI, R., FORNACIARI, E., FRONTALINI, F., GIUSBERTI, L., JOVANE, L., LUCIANI, V., SAVIAN, J. and SPROVIERI, M., 2012. An integrated stratigraphic record of the Palaeocene–lower Eocene at Gubbio (Italy): new insights into the early Palaeogene hyperthermals and carbon isotope excursions. *Terra Nova*, 24: 380–386. <https://doi.org/10.1111/j.1365-3121.2012.01076.x>.
- COCCIONI, R. and PREMOLI-SILVA, I., 2015. Revised Upper Albian–Maastrichtian planktonic foraminiferal biostratigraphy and magnetostratigraphy of the classical Tethyan Gubbio section (Italy). *Newsletters on Stratigraphy*, 48: 47–90. <https://doi.org/10.1127/nos/2015/0055>.
- COCCIONI, R., FRONTALINI, F., CATANZARITI, R., JOVANE, L., RODELLI, D., RODRIGUES, I. M. M., SAVIAN, J. F., GIORGIONI, M. and GALBRUN, B., 2019. Paleoenvironmental signature of the Selandian–Thanetian Transition Event (STTE) and Early Late Paleocene Event (ELPE) in the Contessa Road section (western Neo-Tethys). *Palaeogeography, Palaeoclimatology, Palaeoecology*, 523: 62–77. <https://doi.org/10.1016/j.palaeo.2019.03.023>.
- DARVISHZAD, B., GHASEMI-NEJAD, E., GHOURCHAEI, S. and KELLER, G., 2007. Planktonic foraminiferal biostratigraphy and faunal turnover across the K/Pg boundary in southwestern Iran. *Journal of Science of University of Tehran*, 18: 139–149; (in Persian, with English abstract).
- ETEMAD, M., VAZIRI-MOGHADAM, H., AMIRI BAKHTIAR, H. and RAHMANI, A., 2008. Biostratigraphy and Bathymetry of the Gurpi Formation in Lar Area (Kuh-e-Gach), Based on Planktonic Foraminifera. *Esfahan University Research Journal (Science)*, 32: 57–68; (in Persian, with English abstract).
- EZAMPANAH, Y., SCOPELLITI, G., SADEGHI, A., JAMALI, A. M., YAZDI-MOGHADAM, M. and KAMYABI SHADAN, H., 2018. Biostratigraphy and isotope stratigraphy of upper Maastrichtian–Danian marine deposits of the Kopet-Dagh Basin, northeast Iran. *Cretaceous Research*, 90: 97–114. <https://doi.org/10.1016/j.cretres.2018.03.011>.
- FAROUK, S., 2014. Maastrichtian carbon cycle changes and planktonic foraminiferal bioevents at Gebel Matulla, west-central Sinai, Egypt. *Cretaceous Research*, 50: 238–251. <https://doi.org/10.1016/j.cretres.2014.02.021>.
- FAROUK, S. and FARIS, M., 2012. Late Cretaceous calcareous nannofossil and planktonic foraminiferal bioevents of the shallow-marine carbonate platform in the Mitla Pass, west central Sinai, and Egypt. *Cretaceous Research*, 33: 50–65. <https://doi.org/10.1016/j.cretres.2011.08.002>.
- FAROUK, S., THIBAUT, N., JAFF, R. B. N., FARIS, M., AHMAD, F. and KHASHABA, A., 2018. An integrated study of upper Campanian–lower Maastrichtian carbon isotopes and calcareous plankton biostratigraphy of the Kurdistan Region, northeastern Iraq. *Cretaceous Research*, 82: 64–80. <https://doi.org/10.1016/j.cretres.2017.09.020>.
- FOROUGH, F. and ARYANASAB, M. R., 2018. Biostratigraphy and paleoecology of Calcareous nannofossils from upper Gurpi and base of Pabdeh formations in Kuh-e Gurpi anticline, Zagros Basin, SW of Iran for demonstration of K/Pg boundary. In: The 36th National and the 3rd International Geosciences Congress, Tehran, Iran, 1–8.
- GHASEMI-NEJAD, E., HOBBI, M. H. and SCHIOLER, P., 2006. Dinoflagellate and foraminiferal biostratigraphy of the Gurpi Formation (Upper Santonian–Upper Maastrichtian), Zagros Mountains, Iran. *Cretaceous Research*, 27: 828–835. <https://doi.org/10.1016/j.cretres.2006.03.013>.



- GUASTI, E., SPEIJER, R. P., BRINKHUIS, H., SMIT, J. and STEUR-BAUT, E., 2006. Paleoenvironmental change at the Danian–Selandian transition in Tunisia: foraminifera, organic-walled dinoflagellate cyst and calcareous nannofossil records. *Marine Micropaleontology*, 59: 210–229.  
<https://doi.org/10.1016/j.marmicro.2006.02.008>.
- HADAVI, F. and SENEMARI, S., 2010. Calcareous nannofossils from the Gurpi Formation (Lower Santonian-Maastrichtian), faulted Zagros range, western Shiraz, Iran. *Stratigraphy and Geological Correlation*, 18: 166–178.  
<https://doi.org/10.1134/S086959381002005X>.
- HEMMATI-NASAB, M., GHASEMI-NEJAD, E. and DARVISHZAD, B., 2008. Paleobathymetry of the Gurpi Formation based on benthic and planktonic foraminifera in Southwestern Iran. *Journal of Science of University of Tehran*, 34: 157–173. (in Persian, with English abstract).
- JAMES, G. A. and WYND, J. G., 1965. Stratigraphy Nomenclature of Iranian Oil Consortium Agreement Area. *American Association of Petroleum Geologist Bulletin*, 49: 2182–2245.
- JIANG, M. J. and GARTNER, S., 1986. Calcareous nannofossil succession across the Cretaceous-Tertiary boundary in east-central Texas. *Micropaleontology*, 32: 232–255.
- KAMALI, M. R., FATHI MOBARAKABAD, A. and MOHSENIAN, E., 2006. Petroleum geochemistry and thermal modeling of Pabdeh Formation in Dezful Embayment. *Journal of Science of University of Tehran*, 32: 1–11; (in Persian, with English abstract).
- KELLER, G., 2004. Low-diversity, late Maastrichtian and early Danian planktic foraminiferal assemblages of the eastern Tethys. *Journal of Foraminiferal Research*, 34: 49–73.  
<https://doi.org/10.2113/0340049>.
- KELLER, G., BHOWMICK, P. K., UPADHYAY, H., DAVE, A., REDDY, A. N., JAIPRAKASH, B. C. and ADATTE, T., 2011. Deccan volcanism linked to the Cretaceous-Tertiary boundary mass extinction: new evidence from ONGC wells in the Krishna-Godavari Basin. *Journal of the Geological Society of India*, 78: 399–428.  
<https://doi.org/10.1007/s12594-011-0107-3>.
- KHALIL, H. and AL SAWY, S., 2014. Integrated biostratigraphy, stage boundaries and paleoclimatology of the Upper Cretaceous–Lower Eocene successions in Kharga and Dakhla Oases, Western Desert, Egypt. *Journal of African Earth Sciences*, 96: 220–242.  
<https://doi.org/10.1016/j.jafrearsci.2014.04.010>.
- KHALIL, H. and ZAHRAN, E., 2014. Calcareous nannofossil biostratigraphy and stage boundaries of the Santonian-Eocene successions in Wadi El Mizeira northeastern Sinai, Egypt. *International Journal of Geosciences*, 5: 432–449.  
<http://doi.org/10.4236/ijg.2014.54041>.
- MARTINI, E., 1971. Standard Tertiary and Quaternary calcareous nannoplankton zonation. In: Farinacci, A., Eds., *Proceedings of the 2nd Planktonic Conference*, 2: 739–785. Rome: Tecnoscienza.
- MATEO, P., KELLER, G., PUNEKAR, J. and SPANGENBERG, J. E., 2017. Early to Late Maastrichtian environmental changes in the Indian Ocean compared with Tethys and South Atlantic. *Palaeogeography, Palaeoclimatology, Palaeoecology*, 478: 121–138.  
<https://doi.org/10.1016/j.palaeo.2017.01.027>.
- MOHAMMADKHANI, H., HOSSEINI-BARZI, M., SADEGHI, A. and POMAR, L., 2022. Middle Miocene short-lived Tethyan seaway through the Zagros foreland basin: Facies analysis and paleo-environmental reconstruction of mixed siliciclastic-carbonate deposits of Mishan Formation, Dezful Embayment, SW Iran. *Marine and Petroleum Geology*, 140: 105649.  
<https://doi.org/10.1016/j.marpetgeo.2022.105649>.
- MOTIEL, H., 1995. Iran Petroleum Geology-Geology of the Zagros 1. Tehran: Geological Survey of Iran, 1009 pp.
- , 2003. *Stratigraphy of Zagros*. Tehran: Geological Survey of Iran, 583 pp.
- NAVABPOUR, P., ANGELIER, J. and BARRIER, E., 2010. Mesozoic extensional brittle tectonics of the Arabian passive margin, inverted in the Zagros collision (Iran, interior Fars). In: Leturmy, P. and Robin, C., Eds., *Tectonic and Stratigraphic Evolution of Zagros and Makran during the Mesozoic–Cenozoic*, 65–94. Geological Society, London, Special Publications.
- OVECHKINA, M. N. and ALEKSEEV, A. S., 2004. Quantitative changes of calcareous nannoflora in the Saratov region (Russian Platform) during the late Maastrichtian warming event. *Journal of Iberian Geology*, 31: 149–165.
- PARANDAVAR, M., MAHANIPOUR, A. and AGHANABATI, S. A., 2013. Biostratigraphy of calcareous nannofossils in the latest Maastrichtian-early Paleocene in the Shaikh makan Section (N plunge of SE Kabir kuh). *Journal of Stratigraphy and Sedimentology*, 1: 59–87. (in Persian, with English abstract).
- PERCH-NIELSEN, K., 1972. Remarks on late Cretaceous to Pleistocene coccoliths from the North Atlantic. *Initial Reports of the Deep Sea Drilling Project*, 12: 1003–1069.
- , 1985a. Mesozoic Calcareous Nannofossils. In: Bolli, H. M., Saunders, J. B. and Perch-Nielsen, K., Eds., *Plankton Stratigraphy*, 329–426. Cambridge University, Cambridge.
- , 1985b. Cenozoic Calcareous Nannofossils. In: Bolli, H.M., Saunders, J.B. and Perch-Nielsen, K., Eds., *Plankton Stratigraphy*, 427–554. Cambridge: Cambridge University Press.
- POSPICHAL, J. J., 1996. Calcareous nannoplankton mass extinction at the Cretaceous/Tertiary boundary: An update. *Geological Society of America Special Papers*, 307: 335–360.  
<https://doi.org/10.1130/0-8137-2307-8.335>.
- RAFFI, I. and BACKMAN, J., 2022. The role of calcareous nannofossils in building age models for Cenozoic marine sediments: a review. *Rendiconti lincei. scienze fisiche e naturali*, 33: 25–38.  
<https://doi.org/10.1007/s12210-022-01048-x>
- RAZMJOOEI, M. J., THIBAUT, N., KANI, A., MAHANIPOUR, A., BOUSSAHA, M. and KORTE, C., 2014. Coniacian–Maastrichtian calcareous nannofossil biostratigraphy and carbon-isotope stratigraphy in the Zagros Basin (Iran): consequences for the correlation of Late Cretaceous Stage Boundaries between the Tethyan and Boreal realms. *Newsletters on Stratigraphy*, 47: 183–209.  
<https://doi.org/10.1127/0078-0421/2014/0045>.
- RAZMJOOEI, M. J., THIBAUT, N., KANI, A., DINARÈS-TURELL, J., PUCEAT, E., SHAHRIARI, S., RADMACHER, W., JAMALI, A. M., ULLMANN, C. V., VOIGT, S. and COCQUEREZ, T., 2018. Integrated bio- and carbon-isotope stratigraphy of the Upper Cretaceous Gurpi Formation (Iran): a new reference for the eastern Tethys and its implications for large-scale correlation of stage boundaries. *Cretaceous Research*, 91: 312–340.  
<https://doi.org/10.1016/j.cretres.2018.07.002>.
- RENNE, P. R., DEINO, A. L., HILGEN, F. J., KUIPER, K. F., MARK, D. F., MITCHELL, W. S., MORGAN, L. E., MUNDIL, R. and SMIT, J., 2013. Time scales of critical events around the Cretaceous–Paleogene boundary. *Science*, 339: 684–687.  
<https://doi.org/10.1126/science.1230492>.

- ROSTAMI, M., LECKIE, M., FONT, E., FRONTALINI, F., FINKELSTEIN, D. B. and KOEBERL, C., 2018. The Cretaceous-Paleogene transition at Galanderud (northern Alborz, Iran): a multidisciplinary approach. *Palaeogeography, Palaeoclimatology, Palaeoecology*, 493: 82–101. <https://doi.org/10.1016/j.palaeo.2018.01.001>.
- ROSTAMI, M., FRONTALINI, F., LECKIE, M., COCCIONI, R., FONT, E. and BALMAKI, B., 2020. Benthic foraminifera across the Cretaceous/Paleogene boundary in the eastern Tethys (northern Alborz, Galanderud section): extinction pattern and paleoenvironmental reconstruction. *Journal of Foraminiferal Research*, 50: 24–50. <https://doi.org/10.2113/gsjfr.50.1.25>.
- ROTH, P. H., 1978. Cretaceous nannoplankton biostratigraphy and oceanography of the Northwestern Atlantic Ocean. *Initial Reports Deep Sea Drilling Project*, 44: 731–59. <https://doi.org/10.2973/DSDP.PROC.44.134.1978>.
- SCHMITZ, B., PUJALTE, V., MOLINA, E., et al. 2011. The global stratotype sections and points for the bases of the Selandian (Middle Paleocene) and Thanetian (Upper Paleocene) stages at Zumaia, Spain. *Episodes*, 34: 220–243. <https://doi.org/10.18814/2011/v34i4/002>.
- SENEMARI, S., 2017. Calcareous nannofossils biostratigraphy of the Gurpi Formation at Kalchenar section in northwest of Izeh. *Geosciences*, 26: 287–294. (in Persian, with English abstract). <https://doi.org/10.22071/gsj.2017.46606>.
- , 2018. Biostratigraphy of Mesozoic-Cenozoic boundary based on calcareous nannofossils in section Bulfars, Southwest Iran. *Iranian Journal of Geology*, 12: 1–9. (in Persian, with English abstract).
- SENEMARI, S. and AZIZI, M., 2012. Nannostratigraphy of the Gurpi Formation (Cretaceous-Tertiary Boundary), in Zagros Basin, Southwestern Iran. *World Applied Science Journal*, 17: 205–210.
- SENEMARI, S. and FOROGHI, F., 2019. Calcareous nannofossil biostratigraphy of the Campanian-Danian interval, Gurpi Formation in the Zagros Basin Southwest Iran. *Geopersia*, 9: 251–264. <https://doi.org/10.22059/GEOPE.2019.269957.648432>.
- SENEMARI, S. and AFGHAH, F., 2020. Biostratigraphic correlation of Santonian-Maastrichtian calcareous nannofossil biozones with planktonic foraminifera zonation, Interior Fars region of the Zagros, southwest Iran. *Carbonates and Evaporites*, 35 (2): 32. <https://doi.org/10.1007/s13146-020-00557-w>.
- SENEMARI, S., FAZLI, L. and OMRANI, M., 2010. The study of calcareous nannofossils correlation and foraminifera planktonic of Gurpi Formation in east of Behbahan. *Geosciences*, 19: 119–126; (in Persian, with English abstract).
- SHERKATI, S. H. and LETOUZEY, J., 2004. Variation of structural style and basin evolution in the Central Zagros (Izeh zone and Dezful Embayment), Iran. *Marine and Petroleum Geology*, 21: 535–554. <https://doi.org/10.1016/j.marpetgeo.2004.01.007>.
- SISSINGH, W., 1977. Biostratigraphy of Cretaceous calcareous nannoplankton. *Geologie en Mijnbouw*, 56: 37–65.
- TANTAWY, A., 2003. Calcareous nannofossil biostratigraphy and paleoecology of the Cretaceous-Tertiary transition in the central eastern desert of Egypt. *Marine Micropaleontology*, 47: 323–356. [https://doi.org/10.1016/S0377-8398\(02\)00135-4](https://doi.org/10.1016/S0377-8398(02)00135-4).
- THIBAULT, N., 2017. Comment on “Extinction, dissolution, and possible ocean acidification prior to the Cretaceous/Paleogene (K/Pg) boundary in the tropical Pacific”. *Palaeogeography, Palaeoclimatology, Palaeoecology*, 506: 260–262. <https://doi.org/10.1016/j.palaeo.2017.11.054>.
- THIBAULT, N. and GARDIN, S., 2010. The calcareous nannofossil response to the end-Cretaceous warm event in the Tropical Pacific. *Palaeogeography, Palaeoclimatology, Palaeoecology*, 291: 239–252. <https://doi.org/10.1016/j.palaeo.2010.02.036>.
- THIBAULT, N., GALBRUN, B., GARDIN, S., MINOLETTI, F. and LE CALLONNEC, L., 2016. The end-Cretaceous in the southwestern Tethys (Elles, Tunisia): orbital calibration of paleoenvironmental events before the mass extinction. *International Journal of Earth Sciences*, 105: 771–795. <https://doi.org/10.1007/s00531-015-1192-0>.
- VELLEKOOP, J., WOELDERS, L., AÇIKALIN, S., SMIT, J., VAN DE SCHOOTBRUGGE, B., OMER YILMAZ, I., BRINKHUIS, H. and SPEIJER, R. P., 2017. Ecological response to collapse of the biological pump following the mass extinction at the Cretaceous-Paleogene boundary. *Biogeosciences*, 14: 885–900. <https://doi.org/10.5194/bg-14-885-2017>.
- WATKINS, D. K., 2007. Quantitative analysis of the calcareous nannofossil assemblages from CIROS-1, Victoria Land Basin, Antarctica. *Journal of Nannoplankton Research*, 29: 130–137.
- WILMSEN, M., FÜRSICH, F. T. and MAJIDIFARD, M. R., 2015. An overview of the Cretaceous stratigraphy and facies development of the Yazd Block, western Central Iran. *Journal of Asian Earth Sciences*, 102: 73–91; <https://doi.org/10.1016/j.jseas.2014.07.015>.
- ZIEGLER, M. A., 2001. Late Permian to Holocene paleofacies evolution of the Arabian plate and its hydrocarbon occurrences. *GeoArabia*, 6: 445–504. <https://doi.org/10.2113/geoarabia0603445>.

APPENDIX 1

Species list.

- 
- Arkhangelskiella cymbiformis* Vekshina 1959  
*Arkhangelskiella maastrichtiensis* Burnett 1997  
*Aspidolithus parvus expansus* (Wise and Watkins) Perch-Nielsen 1984  
*Biantholithus sparsus* Bramlette and Martini 1964  
*Braarudosphaera bigelowii* (Gran and Braarud 1935) Deflandre 1947  
*Calculites obscurus* (Deflandre 1959) Prins and Sissingh in Sissingh (1977)  
*Ceratolithoides aculeus* (Stradner 1961) Prins and Sissingh in Sissingh 1977  
*Chiasmolithus bidens* (Bramlette and Sullivan 1961) Hay and Mohler 1967  
*Chiasmolithus consuetus* (Bramlette and Sullivan 1961) Hay and Mohler 1967  
*Chiasmolithus danicus* (Brotzen 1959) Hay and Mohler 1967  
*Chiastozygus platyrhethus* Hill (1976)  
*Coccolithus pelagicus* (Wallich 1877) Schiller 1930  
*Coccolithus subpertusa* Hay and Mohler 1967  
*Cruciplacolithus primus* Perch-Nielsen 1977  
*Cruciplacolithus tenuis* (Stradner 1961) Hay and Mohler in Hay et al. 1967  
*Discoaster mohleri* Bramlette and Percival 1971  
*Eiffellithus gorkae* Reinhardt (1965)  
*Eiffellithus turriseiffelii* (Deflandre in Deflandre and Fert 1954) Reinhardt (1965)  
*Ellipsolithus macellus* (Bramlette and Sullivan 1961) Sullivan (1964)  
*Ericsonia robusta* (Bramlette and Sullivan 1961) Edwards and Perch-Nielsen 1975  
*Fasciculithus tympaniformis* Hay and Mohler in Hay et al. 1967  
*Heliolithus cantabriae* Perch-Nielsen (1971)  
*Heliolithus kleinpellii* Sullivan 1964  
*Lithraphidites carniolensis* Deflandre 1963  
*Lucianorhabdus cayeuxii* Deflandre 1959  
*Lucianorhabdus maleformis* Reinhardt 1966  
*Lithraphidites quadratus* Bramlette and Martini 1964  
*Markalius inversus* (Deflandre in Deflandre and Fert 1954) Bramlette and Martini 1964  
*Microrhabdulus belgicus* Hay and Towe 1963  
*Microrhabdulus decoratus* Deflandre 1959  
*Micula concava* (Stradner in Martini and Stradner 1960) Verbeek 1976  
*Micula cubiformis* Forchheimer (1972)  
*Micula decussata* Vekshina (1959)  
*Micula murus* (Martini 1961) Bukry 1973  
*Micula praemurus* (Bukry 1973) Stradner and Steinmetz 1984  
*Micula prinsii* Perch-Nielsen 1979  
*Micula swastica* Stradner and Steinmetz (1984)  
*Neococcolithes protenus* (Bramlette and Sullivan 1961) Black 1967  
*Placozygus sigmoides* (Bramlette and Sullivan 1961) Romein 1979  
*Prediscosphaera cretacea* (Arkhangelsky 1912) Gartner 1968  
*Prinsius bisulcus* (Stradner 1963) Hay and Mohler 1967  
*Prinsius martinii* (Perch-Nielsen 1969) Haq 1971  
*Prinsius tenuiculus* (Okada and Thierstein 1979) Perch-Nielsen 1984  
*Rhagodiscus angustus* (Stradner 1963) Reinhardt 1971  
*Reinhardtites levis* Prins and Sissingh in Sissingh 1977  
*Sphenolithus moriformis* (Brönnimann and Stradner 1960) Bramlette and Wilcoxon 1967  
*Sphenolithus primus* Perch-Nielsen (1971)  
*Sphenolithus anarrhopus* Bukry and Bramlette 1969  
*Tetrapodorhabdus decorus* (Deflandre in Deflandre and Fert 1954) Wind and Wise 1983  
*Thoracosphaera operculata* Bramlette and Martini (1964)  
*Watznaueria barnesiae* (Black in Black and Barnes 1959) Perch-Nielsen (1968)  
*Watznaueria biporta* Bukry 1969